Research Article | Vol. 24, No. 22 | 31 Oct 2016 | OPTICS EXPRESS 25697

Optics EXPRESS

Infrared glass-based negative-curvature anti-resonant fibers fabricated through extrusion

RAFAEL R. GATTASS,[1,*] DANIEL RHONEHOUSE,[2] DANIEL GIBSON,[1] COLLIN C.MCCLAIN,[2] RAJESH THAPA,[3] VINH Q. NGUYEN,[1] SHYAM S. BAYYA,[1] R. JOSEPH WEIBLEN,[4] CURTIS R. MENYUK,[4] L. BRANDON SHAW,[1] AND JASBINDER S. SANGHERA[1]

[1]*U.S. Naval Research Laboratory, 4555 Overlook Ave SW., Washington, DC 20375, USA*
[2]*University Research Foundation, 6411 Ivy Ln Suite 110, Greenbelt, Maryland 20770, USA*
[3]*Sotera Defense Solutions, 2121 Cooperative Way Suite 400, Herndon, Virginia 20171, USA* [4]*University of Maryland Baltimore County, Baltimore, Maryland 21250, USA*
[*]*rafael.gattass@nrl.navy.mil*

Abstract: Negative curvature fibers have been gaining attention as fibers for high power infrared light. Currently, these fibers have been made of silica glass and infrared glasses solely through stack and draw. Infrared glasses' lower softening point presents the opportunity to perform low-temperature processing methods such as direct extrusion of pre-forms. We demonstrate an infrared-glass based negative curvature fiber fabricated through extrusion. The fiber shows record low losses in 9.75 – 10.5 µm range (which overlaps with the CO_2 emission bands). We show the fiber's lowest order mode and measure the numerical aperture in the longwave infrared transmission band. The possibility to directly extrude a negative curvature fiber with no penalties in losses is a strong motivation to think beyond the limitations of stack-and-draw to novel shapes for negative curvature fibers.

OCIS codes: (060.2390) Fiber optics, infrared; (060.2280) Fiber design and fabrication.

References and links

1. F. Benabid and P. J. Roberts, "Linear and nonlinear optical properties of hollow core photonic crystal fiber," J. Mod. Opt. **58**(2), 87–124 (2011).
2. J. Harrington, "A review of IR transmitting, hollow waveguides," Fiber Integr. Opt. **19**(3), 211–227 (2000).
3. A. D. Pryamikov, A. S. Biriukov, A. F. Kosolapov, V. G. Plotnichenko, S. L. Semjonov, and E. M. Dianov, "Demonstration of a waveguide regime for a silica hollow--core microstructured optical fiber with a negative curvature of the core boundary in the spectral region > 3.5 µm," Opt. Express **19**(2), 1441–1448 (2011).
4. F. Yu and J. C. Knight, "Negative curvature hollow-core optical fiber," IEEE J. Sel. Top. Quantum Electron. **22**(2), 146–155 (2016).
5. F. Couny, F. Benabid, P. J. Roberts, P. S. Light, and M. G. Raymer, "Generation and photonic guidance of multi-octave optical-frequency combs," Science **318**(5853), 1118–1121 (2007).
6. L. Vincetti, "Empirical formulas for calculating loss in hollow core tube lattice fibers," Opt. Express **24**(10), 10313–10325 (2016).
7. L. Vincetti and V. Setti, "Waveguiding mechanism in tube lattice fibers," Opt. Express **18**(22), 23133–23146 (2010).
8. A. N. Kolyadin, A. F. Kosolapov, A. D. Pryamikov, A. S. Biriukov, V. G. Plotnichenko, and E. M. Dianov, "Light transmission in negative curvature hollow core fiber in extremely high material loss region," Opt. Express **21**(8), 9514–9519 (2013).
9. A. F. Kosolapov, A. D. Pryamikov, A. S. Biriukov, V. S. Shiryaev, M. S. Astapovich, G. E. Snopatin, V. G. Plotnichenko, M. F. Churbanov, and E. M. Dianov, "Demonstration of CO2-laser power delivery through chalcogenide-glass fiber with negative-curvature hollow core," Opt. Express **19**(25), 25723–25728 (2011).
10. V. S. Shiryaev, A. F. Kosolapov, A. D. Pryamikov, G. E. Snopatin, M. F. Churbanov, A. S. Biriukov, T. V. Kotereva, S. V. Mishinov, G. K. Alagashev, and A. N. Kolyadin, "Development of technique for preparation of As_2S_3 glass preforms for hollow core microstructured optical fibers," J. Optoelectron. Adv. Mater. **16**, 1020–1025 (2014).
11. G. Tao, H. Ebendorff-Heidepriem, A. M. Stolyarov, S. Danto, J. V. Badding, Y. Fink, J. Ballato, and A. F. Abouraddy, "Infrared fibers," Adv. Opt. Photonics **7**(2), 379–458 (2015).
12. K. M. Kiang, K. Frampton, T. M. Monro, R. Moore, J. Tucknott, D. W. Hewak, D. J. Richardson, and H. N. Rutt, "Extruded single mode non-silica glass holey optical fibres," Electron. Lett. **38**(12), 546–547 (2002).

#273997 http://dx.doi.org/10.1364/OE.24.025697
Journal © 2016 Received 16 Aug 2016; revised 19 Sep 2016; accepted 29 Sep 2016; published 26 Oct 2016

13. H. Ebendorff-Heidepriem and T. M. Monro, "Extrusion of complex preforms for microstructured optical fibers," Opt. Express **15**(23), 15086–15092 (2007).
14. H. Ebendorff-Heidepriem, T.-C. Foo, R. C. Moore, W. Zhang, Y. Li, T. M. Monro, A. Hemming, and D. G. Lancaster, "Fluoride glass microstructured optical fiber with large mode area and mid-infrared transmission," Opt. Lett. **33**(23), 2861–2863 (2008).
15. M. R. Oermann, H. Ebendorff-Heidepriem, D. J. Ottaway, D. G. Lancaster, P. J. Veitch, and T. M. Monro, "Extruded microstructured fiber lasers," IEEE Photonics Technol. Lett. **24**(7), 578–580 (2012).
16. X. Feng, T. M. Monro, P. Petropoulos, V. Finazzi, and D. J. Richardson, "Extruded single-mode high-index-core one-dimensional microstructured optical fiber with high index-contrast for highly nonlinear optical devices," Appl. Phys. Lett. **87**(8), 081110 (2005).
17. D. Furniss and A. B. Seddon, "Towards monomode proportioned fibreoptic preforms by extrusion," J. Non-Cryst. Solids **256–257**, 232–236 (1999).
18. M. Zhu, X. Wang, Z. Pan, C. Cheng, Q. Zhu, C. Jiang, Q. Nie, P. Zhang, Y. Wu, S. Dai, T. Xu, G. Tao, and X. Zhang, "Fabrication of an IR hollow-core Bragg fiber based on chalcogenide glass extrusion," Appl. Phys., A Mater. Sci. Process. **119**(2), 455–460 (2015).
19. Y. Sun, S. Dai, P. Zhang, X. Wang, Y. Xu, Z. Liu, F. Chen, Y. Wu, Y. Zhang, R. Wang, and G. Tao, "Fabrication and characterization of multimaterial chalcogenide glass fiber tapers with high numerical apertures," Opt. Express **23**(18), 23472–23483 (2015).
20. D. J. Gibson and J. A. Harrington, "Extrusion of hollow waveguide preforms with a one-dimensional photonic bandgap structure," J. Appl. Phys. **95**(8), 3895–3900 (2004).
21. J. S. Sanghera and I. D. Aggarwal, eds., *Infrared Fiber Optics* (CRC, 1998).
22. R. J. Weiblen, C. R. Menyuk, R. R. Gattass, L. B. Shaw, and J. S. Sanghera, "Fabrication tolerances in As_2S_3 negative-curvature antiresonant fibers," Opt. Lett. **41**(11), 2624–2627 (2016).
23. P. Klocek, *Handbook of Infrared Optical Materials* (CRC, 1991).
24. B. Temelkuran, S. D. Hart, G. Benoit, J. D. Joannopoulos, and Y. Fink, "Wavelength-scalable hollow optical fibres with large photonic bandgaps for CO_2 laser transmission," Nature **420**(6916), 650–653 (2002).

1. Introduction

The ability of hollow-core fibers to transmit light through air has been a source of much interest for routing high power lasers, routing multiple wavelength bands and signals with wide bandwidth [1]. Beyond metal coated capillaries [2], a new class of hollow-core anti-resonant fibers has been gaining attention based on their geometrical simplicity [3,4]. These "negative curvature" fibers, have consisted mostly of a hollow core surrounded by a circular array of hollow tubes. Light propagating in the core is effectively guided since scattering from the core to any other mode is effectively inhibited [5].

An attractive feature of these negative-curvature fibers is that light can be transmitted in wavelength regions where the fiber material absorption is high, for example beyond the multi-phonon absorption edge. The light is not transmitted along all wavelengths, but rather only for certain wavelength bands that satisfy loosely an anti-resonant condition [4,6,7]. In practice these fibers show multiple transmissions bands, with losses on the order of 1000 times lower than the intrinsic material absorption.

Previous research in silica-based anti-resonant fibers has extended the transmission of these fibers well beyond the material absorption edge (~2.5 μm), and losses less than 1 dB/m at wavelengths in the mid-infrared (2 − 5 μm) have been demonstrated [8]. For fibers targeting the long-wave infrared optical band (8 − 12 μm), natural candidates would be infrared glasses of which there are many alternatives such as fluorides, tellurides and chalcogenides. Previous work in chalcogenide-based anti-resonant fibers has demonstrated transmissions losses on the order of 11 dB/m around the CO_2 laser band [9].

All previous work on negative-curvature anti-resonant fibers has focused on "tube-lattice" type fibers, where the fiber is composed of an array of hollow tubes surrounding a center hollow core. This has been the case not only for experimental work but also, surprisingly, for theoretical work. The enormous success of fabrication methods for photonics crystal and Kagome silica fibers may explain this emphasis. These fibers are normally fabricated through a "stack-and-draw" method where a series of tubes is assembled in a geometrical shape, fused and then drawn down into a fiber. Transitioning from silica to soft glasses presents extra challenges, one of which can be obtaining tubes with high manufacturing tolerances. While

Optics EXPRESS

there are researchers attempting to address the challenges of making the tubes in soft glasses [10], we propose the use of an extrusion method to fabricate these fibers.

In the most common implementation, a bulk piece of soft-glass is heated close to the softening point and pushed through a die to form a preform. The preform is drawn down into a fiber in a second step, where in the glass is heated again and stretched into a fiber. Extrusion has already been used to form photonic crystal fibers in a variety of soft materials, and work in this field was been extensively reviewed in [11]. All established soft-glass systems have had demonstrations of extrusion for the formation of fiber such as silica based glasses [12], bismuth glass and other soft glasses [13], fluoride glass [14], and tellurite glass [15]. The process has even been used to make multiple material soft-glass fibers such as multiple compositions borosilicate glasses [16], multiple chalcogenide compositions [17–19], and multimaterial chalcogenide and polymers [20].

In this paper we take advantage of the ability to process a soft-glass at low temperatures to extrude the preform for a negative curvature fiber directly, a process that is significantly less labor intensity than stacking multiple tubes and bonding them. We show that this approach not only works for making a fiber displaying anti-resonance guiding but that the transmission along this fiber exceeds all previously reported values.

2. Fabrication method

We chose to fabricate our fibers using arsenic sulfide glass due to its high transmission in the mid-infrared range and stability to crystallization, as well as being a well-established material composition for infrared fibers [11,21]. Theoretical estimates for the losses expected for As_2S_3 negative curvature fibers are on the order of 10^{-3} dB/m for mid-infrared wavelengths and 1 dB/m for longwave infrared wavelengths [9,10,22].

The glass was formed from commercial precursors which were purified in controlled atmospheric environments to minimize impurities that contribute to high fiber loss. The high purity precursors are mixed and sealed in evacuated quartz ampoules and melted and quenched to form glasses. Typical melt temperatures for the glasses used were approximately 750°C. The liquids are quenched and the glass rods annealed at temperatures around the softening temperatures ~200 °C.

In order to confirm that the extrusion method could be used to make a high enough quality surface for the fabrication of a negative curvature fiber, we selected an eight ring design similar to the one already demonstrated through stack and draw in silica [8]. The die was fabricated to have a preform of 19.5 mm outer dimension and rings with 3.84 mm outer diameter and 0.46 mm wall thickness.

Extrusions were performed with a custom-designed vertical glass extruder using a 25-mm diameter stainless steel ram and sleeve with no additional sleeve lining. The extruder exit end is equipped with a three-jaw chuck on a motorized slide to allow for positive control of draw speed as the extrusion length and weight increases. Glass samples that were approximately 24.8 mm diameter x 53 mm long were placed inside the stainless sleeve. Extrusions were performed at a die exit temperature of 371 °C, while ram speed and extrusion draw speed were maintained at 0.6 mm/min and 3.15 mm/min respectively. Under these conditions a steady state ram load of approximately 135 kg was obtained during the extrusion process. Preforms produced by this method proved to be highly symmetric with well-defined features. The resulting preform had dimensions of 18 mm outer diameter by ~135 mm length.

Fig. 1. Diamond saw cut extruded preform.

Figure 1 shows the preform produced by the extrusion process after being cut to length to remove any portion of the ends with irregularities, tapering or closed holes. However, the extruded preform end-face still shows that small variations among internal tubes. Control over the inner tube dimensions will be accomplished in the fiber draw by controlling the relative pressure in all openings of the preform. On one end of the preform, a fluoropolymer tube was inserted in the "core" center opening and epoxied to the preform. This was performed while ensuring none of the inner tubes opening were closed. A glass-tube, three-way valve was attached to the preform to connect all the inner apertures simultaneously, and the center opening separately. This arrangement allowed for the eight inner tubes to be pressurized while the central region was kept at atmospheric pressure. The glass was heated to approximately 290 °C and drawn to fiber. The pressure applied to the either inner tube pressured was varied along in the fiber draw in 5 mBar increments from 30 to 60 mBar using He gas. Figure 2 shows the evolution of the fiber holes as a function of pressure. At a pressure of 35 mBar initial expansion of the inner tubes began to occur with maximum expansion without the tubes coming into contact with each other occurring at ~40mBar.

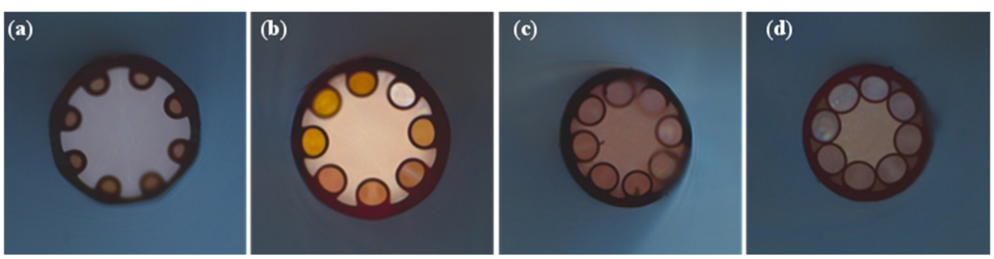

Fig. 2. Drawn fiber with different inner tube pressures. (a) 0 mBar, (b) 35 mBar, (c) 40 mBar and (d) 45 mBar. At 45 mBar the eight inner tubes expand to the point of contact with each other.

Figure 3(a) shows a confocal microscope image of the end face of drawn fiber. The roughness observed in the image is solely caused by the cleaving of the fiber. The fiber was mechanically strong even without any polymer coating, emphasizing the high stability of As_2S_3 glass to crystallization. As can be observed in Fig. 3(a), the fiber is not perfectly symmetric, displaying some variance on the dimensions of the outer diameter tubes, gaps and thickness. Table 1 summarizes the average dimensions and the standard deviations.

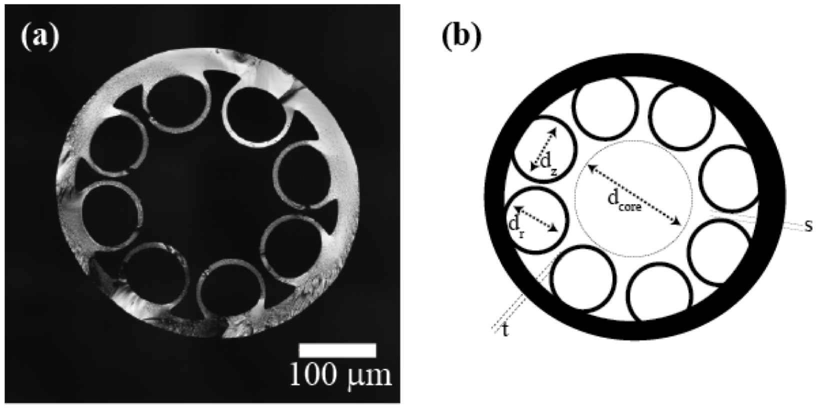

Fig. 3. (a) Confocal microscope image of the As_2S_3 Negative curvature fiber cleaved end face. (b) cartoon showing the various dimensions in Table 1.

Table 1. Average dimensions for negative curvature fiber in Fig. 3.

	Average (µm)	Standard deviation (µm)
d_z: inner tube diameter azimuthal	70.8	5.5
d_r: inner diameter radial	75.1	4.2
t: inner tube wall thickness	7.0	0.5
s: inner tube spacing	9.0	3.1
d_{core}: core diameter	172.4	9.4

3. Fiber characterization

Fiber transmission losses for wavelengths across the infrared region were determined by the cut-back method. A nitrogen purged Fourier-transform infrared spectrometer was used to measure the losses. Figure 4 shows the loss in dB/m for the fiber shown in Fig. 3. Light was coupled into the fiber with a 25.4 cm radius of curvature gold coated elliptical mirror and collected into a liquid nitrogen cooled detector with 25.4 radius of curvature gold coated elliptical mirror. The large peak around 4 µm is associated with the intrinsic absorption of H-S and is expected from an unpurified glass. For comparison the transmission edges for a standard As_2S_3 are plotted as red dashed lines in the chart. The fiber transmission in the 2 – 5 µm window (MWIR) while being on the same order of magnitude as a that of a solid-core chalcogenide fibers is about 3 times higher, while in the 8 – 12 µm (LWIR) range a transmission window in the 9.5 – 11.5 µm range is clearly observed. In this LWIR range the losses reach a minimum of 2.1 dB/m at 10.0 µm. This is significantly below the measured transmission loss for a bulk piece of As_2S_3 which is on the order of 380 dB/m [23]. As a reference, Fig. 4b shows the measured transmission loss of our fiber in the 8 – 12 µm compared to other chalcogenide anti-resonant fibers in this range.

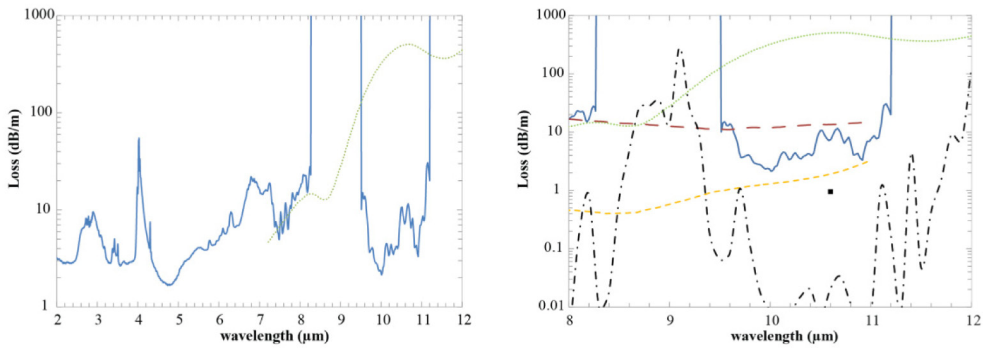

Fig. 4. (a) (solid line) Transmission loss (dB/m) for the fiber shown in Fig. 3, (green dotted line) Bulk As_2S_3 transmission according to [23]. (b) Comparison of transmission loss for extruded fiber (solid line), bulk As_2S_3 transmission according to [23] (green dotted line), chalcogenide glass negative curvature fiber from [9] (red dashed line), typical GeAsSeTe solid core fiber drawn at NRL (yellow dashed line), hollow core ommniguide fiber [24] (square dot) and (black dashed-dotted line) calculated transmission.

Once the LWIR transmission windows were determined, a quantum cascade laser was used to test the transmission around the LWIR transmission band. A 25.4 mm focal length lens was used to couple the free-space beam from a tunable quantum cascade laser into a 2-m long fiber piece. The output mode was measured with a pyroelectric camera. Figure 5 shows the output beam at 9.8 µm wavelength.

The same setup was used to measure the output numerical aperture of the fiber. A series of images were taken for increasing distances from the fiber and the beam divergence was fit as a function of the distance to determine the numerical aperture. The numerical aperture at 9.2 µm wavelength was determined to be 0.036 and 0.027 for the radial and azimuthal axis respectively. These values are on the order of half the numerical aperture of the input imaging system.

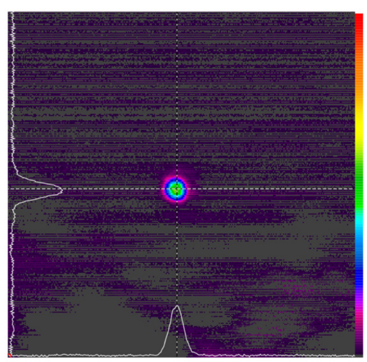

Fig. 5. Output beam after propagation through 2-m of fiber at 9.8 µm wavelength. Image was captured with a thermo-electric camera positioned a distance of 25.4 mm from the fiber.

4. Numerical calculation for fiber

As shown in Fig. 3, the resulting fiber structure is not a series of perfectly matched tubes, but in reality it presents fluctuations in sizes and thicknesses of the tubes. A perfectly symmetric set of tubes with various tube thickness were simulated and the losses for the HE_{11} mode were determined from the imaginary part of the refractive index. The fiber outer clad was surrounded by a perfectly matched layer outside the fiber to simulate confinement loss. The finite-element mesh had six elements per wavelength in the air regions and 16 elements per wavelength in the As_2S_3 regions. The best match for the LWIR transmission band was

Optics EXPRESS

obtained for a tube of 6.4 μm thickness and the resulting transmission bands are shown in Fig. 4b as dashed-dotted lines.

5. Discussion

The use of a soft-glass such as the sulfide-based chalcogenide glass presented in this work is particularly important for the LWIR optical band. Research has mainly focused in anti-resonant silica fibers, demonstrating that light can be transmitted with acceptable losses in an optical window beyond the materials intrinsic absorption limit such as MWIR light transmission with < 1 dB/m loss [8]. Research in anti-resonant sulfide-based fibers based on stack and draw, already demonstrated losses of 11 dB/m near the 9.5 μm CO_2 line [9]. Here we demonstrate that we can make use of both advantages of the soft glass, the improved transmission in the infrared and the flexibility in fabricating through extrusion. However, this is accomplished with no transmission penalty as the measured loss in the LWIR (near the CO_2 lines) is actually the lowest transmission loss ever recorded for a negative curvature in this range.

Moreover, the measured transmission loss has been determined through a cut-back method with an FTIR. As has been acknowledged by other researchers [10], this does not properly reflect the losses of the fiber in a realistic use scenario. The FTIR light excitation will excite many other modes beyond the fundamental HE_{11} low loss mode, and therefore the measured loss only represents an upper bound for the transmission loss. Lower loss is expected for light excitation at the proper numerical aperture, for a mode matched mode.

A limitation of the current work has been the accuracy with which we could fabricate the final structure. For stack-and-draw fabricated structures, there is an established commercial base from which one can secure tubes with tight tolerances (for silica), and the same is slowly becoming true for soft glasses with an increasing number of vendors entering the field. However, the tube must still be bonded to the outer jacket, something that can be challenging for materials with sharp viscosity curves as is the case for soft glasses. Extruding a preform from a soft glass immediately bypasses this limitation. In our work, although the fiber displays anti-resonant transmission bands, the fiber did have a large variance in the features. We have recently reported on the increased loss expected for variations in the thickness and gap spacing in anti-resonant fibers [22], and believe that losses for fibers made beyond this initial demonstration should be significantly lower.

As expected fabrication imperfections manifest themselves as increased losses for the fibers [22]. The current theoretical modeling approximates the experimentally observed losses, displaying the LWIR transmission window around 10 μm. The agreement remains qualitative, with the theoretical losses being about two orders of magnitude lower. This result is consistent with the expectation that the presence of imperfections will lead to “blurring” of the transmission bands as described in [22].

6. Conclusion

All negative curvature fibers that have been fabricated to date use a set of tubes that are manually assembled into a preform and then drawn into a fiber. This approach, besides being time-consuming and labor intensive, is strongly restricts the configurations that can be fabricated. The use of extrusion for the fabrication of negative curvature anti-resonant fibers enables a vast new range of structures to be studied. As we show, this method can be used to make current “tube-like” fibers with record low losses, which should be a strong motivation for the broader theoretical community to think beyond the current designs of these fibers.